Auroral production of nitric oxide measured by the SNOE satellite

Stanley C. Solomon and Charles A. Barth

Laboratory for Atmospheric and Space Physics, University of Colorado, Boulder, Colorado

Scott M. Bailey

Center for Atmospheric Sciences, Hampton University, Hampton, Virginia

Abstract. Measurements by the Student Nitric Oxide Explorer (SNOE) satellite ultraviolet spectrometer confirm that nitric oxide density is elevated in the polar thermosphere. Contemporaneous measurements by the SNOE auroral photometer are used to obtain an indication of auroral activity by measuring the equatorward boundary of the auroral oval, and deriving the position of that boundary at midnight magnetic local time. Using these measurements, nitric oxide variability at high latitude is shown to be strongly correlated with auroral activity, with a lag of approximately one day.

Introduction

Nitric oxide density in the terrestrial thermosphere is higher in the polar regions than at middle and tropical latitudes. This has long been thought to be due to auroral generation of nitric oxide (NO), both through direct particle impact that has the ultimate effect of dissociating nitrogen molecules into excited nitrogen atoms, and through heating that accelerates the chemical reactions that create NO from those atoms. The theoretical relationship between the aurora and NO has been investigated [e.g., *Siskind et al.,* 1989] and measurements by AE [*Cravens and Stewart,* 1978], SME [*Barth,* 1992; 1996], HALOE [*Siskind et al.,* 1998], and MAHRSI [*Stevens et al.,* 1997] have demonstrated the high-latitude enhancement of NO. SME and HALOE data have been analyzed to obtain statistical maps for quiet and disturbed conditions [*Siskind et al.,* 1998]. *Crowley et al.* [1998] investigated large fluctuations in NO measured by HALOE during the November 1993 space weather special study period. However, the HALOE instrument performs solar occultation measurements, and so cannot obtain daily latitude distributions. SME measurements of NO were made during a few orbits per day, and MAHRSI measurements from STS were performed over a limited period of time.

The auroral NO distribution is clearly complex, due to the long lifetime of NO, particularly at night, and the consequent importance of horizontal and vertical transport. Thermospheric temperatures also respond to auroral forcing, extending to subauroral regions and even to low latitudes. Most important, auroral events are local phenomena, and the specific atmospheric and ionospheric conditions, solar illumination, and magnetic field configuration determine how much NO is produced from any given auroral disturbance.

The goal of the SNOE satellite is to perform new measurements of NO in conjunction with solar and auroral measurements, and to do so with ~100% duty cycle to eliminate longitude and magnetic field sampling bias. A sun-synchronous orbit was chosen to select a constant local solar time of the observations (10:30 – 22:30), simplifying diurnal variability in the analysis. The NO density distribution is measured by the gamma-band fluorescence method, using an ultraviolet spectrometer that scans the limb with the 5 rpm satellite spin. The solar soft x-ray flux is measured by an array of silicon photodiodes coated with metal foil filters. These measurements are described by *Barth et al.* [1999] and *Bailey et al.* [1999]. Overviews of the spacecraft mission and its scientific instrumentation were given by *Solomon et al.* [1996] and *Bailey et al.* [1996]. SNOE was launched on 26 February 1998 and began instrument operations in early March. Here, we present initial measurements of auroral activity by the SNOE auroral photometer, and their relationship to high latitude NO.

Auroral Boundary Measurements

The SNOE auroral photometer (AP) is a two-channel broadband instrument that measures ultraviolet light emitted by the aurora in response to energetic particle precipitation. Each channel consists of a phototube detector, a filter, and a field of view limiter. Both channels have circular fields of view, 11° full-cone. The detectors are Hamamatsu R1081 photomultiplier tubes with MgF_2 windows and CsI photocathodes; channel 1 has a CaF_2 filter and channel 2 has a BaF_2 filter. This produces a bandpass from 125 to 180 nm for channel 1, which is dominated by the allowed OI triplet at 130.4 nm, and from 135 to 180 nm for channel 2, providing a measurement of N_2 LBH bands and the forbidden OI doublet at 135.6 nm. The instrument uses the satellite spin to scan along track, centered on the nadir direction. The data presented here were integrated over a 7° interval, resulting in an effective spatial integration angle of 18° including the field of view. This corresponds to ~140 km along track at auroral altitude. The satellite moves ~90 km per spin, so the spatial resolution of this measurement is ~1° in latitude.

A useful analysis technique for estimation of auroral activity from this type of data is the auroral boundary method. This has been developed for use with DMSP energetic electron data by *Gussenhoven et al.* [1981; 1983] and *Hardy et al.* [1985]. The method delineates the equatorward boundary of the auroral precipitation region in geomagnetic coordinates, and then maps the boundary location to its equivalent position at midnight magnetic local time (MLT) using a statistical relationship for the auroral oval location derived as a function of MLT and geomagnetic activity level from historical DMSP data. This "midnight boundary index" has been shown by these authors to be a good overall indicator of auroral activity and total energy flux, and correlates well with other indices, but is a more direct measure of auroral oval size.

The approach taken with the SNOE AP data was to use the same method as the DMSP analysis, with a similar estimated

equivalent threshold of ~10^7 particles cm^{-2}s^{-1}sr^{-1}, or ~0.1 erg cm^{-2}s^{-1}. The equivalent brightness level depends on the particle energy distribution and is therefore model dependent, but the auroral boundary is usually quite sharp and its position uncertainty with respect to threshold selection is small. Additional error is introduced by the statistical mapping to magnetic midnight, which is done using the relationship
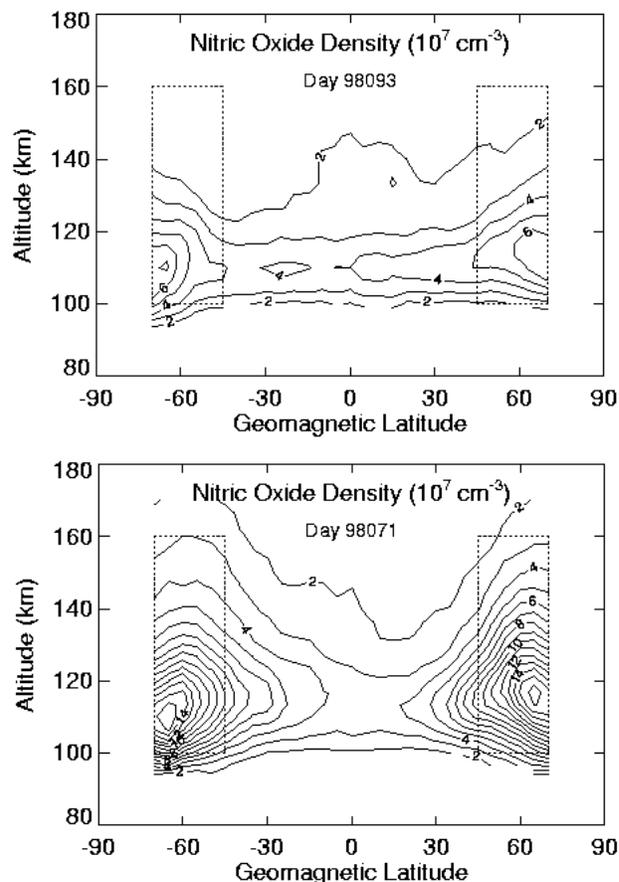
$$\Lambda_M = \alpha_0 + \frac{\alpha_0}{\alpha_i}\left(\Lambda_B - \beta_i\right)$$

derived from *Gussenhoven et al.* [1983], where Λ_B is the measured magnetic latitude boundary in the ith MLT sector, α_i and β_i are the slope and intercept of the fit to the boundary locations in the ith MLT sector as tabulated in that paper at 1-hour intervals, α_0 and β_0 are the slope and intercept for the midnight sector, and Λ_M is the derived midnight boundary magnetic latitude. Fortunately, due to its sun-synchronous orbit, SNOE nighttime auroral transits cover a limited range of MLT, and are never more than a few hours from midnight, so this is a minor adjustment.

Data from the first 81 days of SNOE instrument operations (day 67 to day 147 of 1998) were reduced. Equatorward boundary crossings were obtained from both hemispheres, using channel 1, which has greater response in the ultraviolet and better visible light rejection than channel 2. Boundaries were marked by visual comparison of the data with the estimated threshold values, and crossings where there was any possibility of contamination by dayglow were excluded. A comparison to DMSP particle data is shown in Figure 1, where 3-hour averages of the SNOE midnight boundary are plotted against 3-hours averages of the DMSP midnight boundary index obtained from AFRL data listings. There is some scatter, since the measurements are neither simultaneous nor co-located, but the slope of a linear fit is near unity, with less than half a degree offset at 65°. The correlation coefficient r is 0.85.

This measurement also correlates well with other magnetic-based indices such as the NOAA Hemispheric Power, the Polar Cap Index, and *Kp*. As recently demonstrated [*Knipp et al.,* 1998] midnight boundary indices are good indicators of energy deposition in the auroral thermosphere by Joule heating as well as global levels of particle precipitation and general auroral activity. Therefore, we employ SNOE measurement of the auroral oval midnight boundary in a preliminary analysis of high-latitude NO densities.
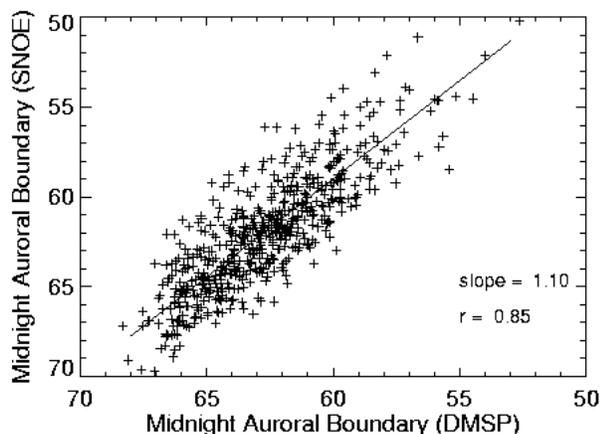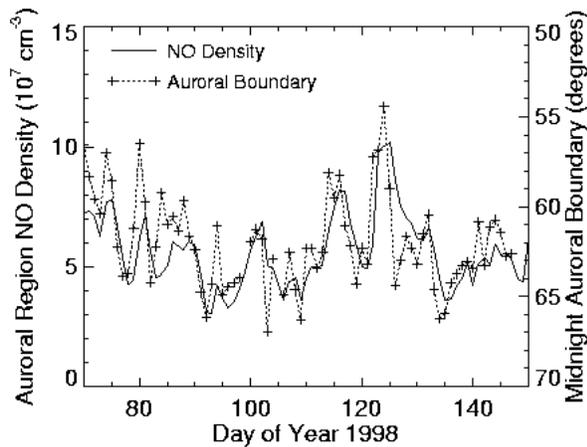

Figure 2. Nitric oxide daily average distributions in magnetic latitude and altitude at 10:30 local solar time, near vernal equinox. The boxes drawn with dotted lines indicate the averaging region used for the comparisons shown in Figures 3 and 4 (100–160 km altitude and 45°–70° magnetic latitude). (*a*) A representative day following a period of quiet geomagnetic conditions (*Ap*=6, previous day *Ap*=4). (*b*) A day following a period of moderately disturbed geomagnetic conditions (*Ap*=12, previous day *Ap*=28).

Nitric Oxide Measurements

Daily averages of the NO density distribution as a function of geomagnetic latitude and altitude are shown in Figure 2. The local solar time of the observations is approximately 10:30. Measurements on a day when magnetic activity was low are shown in Figure 2*a*, and on a day when magnetic activity was high are shown in Figure 2*b*. Both days are near vernal equinox. The change in NO density is striking.

To quantify this change, averages over a large region were taken, extending from 45° to 70° magnetic latitude and from 100 to 160 km altitude, as represented by the boxes drawn on Figure 2. Data from both hemispheres were averaged. This daily average of auroral- to sub-auroral region NO density is plotted in Figure 3 as a function of day number, with daily averages of the SNOE midnight auroral boundary index overplotted. Correspondence between the quantities appears strong, and inspection reveals that changes in NO densities appear to lag changes in the auroral boundary. Therefore, Figure 4 plots NO density as a function of the midnight auroral boundary index with a 1-day lag, i.e., NO density is plotted

Figure 1. Comparison of SNOE and DMSP equatorward midnight auroral boundaries, 3-hour averages for day 67–147 of 1998. A linear fit is shown with the indicated slope and correlation coefficient *r*.
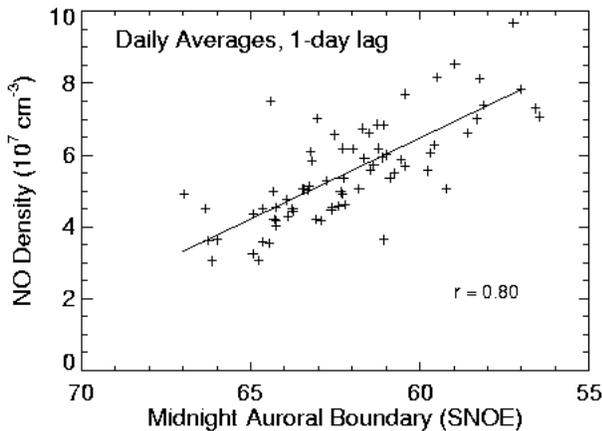
Figure 3. Nitric oxide auroral region daily averages plotted with the SNOE midnight auroral boundary index daily averages.

against the boundary index for the previous day. This results in a systematic relationship represented by the linear fit, with a correlation coefficient r=0.80.

Correlation with other indices of geomagnetic activity and auroral energy input was also performed, as listed in Table 1. All the indices obtain strong correlations, with insignificant differences between them. All are stronger with a 1-day lag than a 0-day or 2-day (or greater) lag. As a control, the $F_{10.7}$ solar radio flux was used, which is a proxy indication of solar EUV and x-ray fluxes. Although significant correlation would be found at low latitude from this index, none was found at high latitude. All correlations were statistically significant (f-tests ranging from 60 to 200) except for $F_{10.7}$.

Discussion

The NO observations are performed during the day, and auroral measurements at night, so the measured NO distribution, albeit aurorally generated at high latitude, is necessarily a photochemically-influenced distribution. A one-day appar-

Figure 4. Nitric oxide auroral region daily averages plotted against the previous day midnight auroral boundary daily averages for the period shown in Figure 3.

Table 1. Matrix of Correlation Coefficients

Daily Average	0-day lag	1-day lag	2-day lag
SNOE Midnight Boundary	0.70	0.80	0.60
DMSP Midnight Boundary	0.75	0.88	0.64
NOAA Hemispheric Power	0.71	0.86	0.65
Polar Cap Index (Thule)	0.69	0.88	0.67
Daily Sum of 3-hour Kp	0.68	0.86	0.66
$F_{10.7}$	0.09	0.05	0.00

ent lag between auroral forcing and resulting changes in NO density is therefore a sensible result. The lifetime of thermospheric NO is approximately half a day, but only under sunlit conditions [Barth, 1992]. Solar ultraviolet and x-rays create NO but also destroy it, primarily through photodissociation. During the polar night, NO can be created by auroral processes, but once the available atomic nitrogen has been consumed by the NO, there are virtually no loss mechanisms. NO therefore persists in an air parcel until transport or rotation of the Earth brings it to a sunlit location. Further, measurement of NO by the fluorescence method is only possible on the day side, so satellite observation of NO changes is additionally delayed. The combination of the lifetime effect and the observational delay should result in a lag of approximately a day. With this lag, auroral region NO is correlated with various auroral particle and geomagnetic indices almost as well as these indices correlate with each other. Thus, tomorrow's nitric oxide is about as good an indicator of today's auroral activity as other global estimates.

Auroral region NO varied by a factor of ~3 during the study period. This is comparable to the factor of ~5 seen at similar altitudes in HALOE data during November 1993 [Crowley et al.,1998]. The change in latitude of the HALOE occultations during that interval may account for some of the observed variation.

The auroral boundary method is a good choice for optical measurements of any type because analysis of the oval interior can be complicated by sunlight. Optical methods generally have that limitation compared to particle detectors, but they also have advantages, including the ability to respond to a wide range of energy, and, when imaging detectors are used, to cover extended spatial regions. The study of partial auroral images for use in analysis and global models may benefit from application of equatorward boundary identification.

Auroral region NO is generated by heating of the atmosphere as well as direct particle impact, particularly by current induced ion-neutral collisions known as Joule heating. This may be important in the ~140–200 km range, where ground-state atomic nitrogen reacting with molecular oxygen becomes an important source of NO. Increases in temperature (and increases in the velocity distribution of atomic nitrogen) accelerate this reaction, and temperature increases can also persist and propagate equatorward. This may be an important mechanism for auroral effects at lower latitude, but its relative importance compared to horizontal transport is not known. These questions and longer-term investigations at higher temporal resolution will be examined in future work with the SNOE measurements.

References

Bailey, S. M., C. A. Barth, M. J. Erickson, R. A. Kohnert, A. W. Merkel, E. M. Rodgers, S. C. Solomon, S. D. Straight, J. E. Vian, and T. N. Woods, Science Instrumentation for the Student Nitric Oxide Explorer, *Proc. SPIE*, *2830*, 264, 1996.

Bailey, S. M., T. N. Woods, C. A. Barth, and S. C. Solomon, Measurements of the solar soft x-ray irradiance from the Student Nitric Oxide Explorer, *Geophys. Res. Lett.*, this issue, 1999.

Barth, C.A., Nitric Oxide in the lower thermosphere, *Planet. Space Sci.*, *40*, 315, 1992.

Barth, C.A., Reference models for thermospheric nitric oxide, *Adv. Space Res., 18*, 179, 1996.

Barth, C. A., S. M. Bailey, and S. C. Solomon, Solar-terrestrial coupling: Solar soft x-rays and thermospheric nitric oxide, *Geophys. Res. Lett.*, this issue, 1999.

Cravens, T. E., and A. I. Stewart, Global morphology of nitric oxide in the lower *E* region, *J. Geophys. Res.*, *83*, 2446, 1978.

Crowley, G., A. Ridley, D. Winningham, R. Frahm, J. Sharber, and J.Russell, Nitric oxide variations in the mesosphere and lower thermosphere during the November 1993 storm period, *J. Geophys. Res.*, *103*, 26395, 1998.

Fuller-Rowell, T. J., and D. S. Evans, Height-integrated Pedersen and Hall conductivity patterns inferred from the TIROS-NOAA satellite data, *J. Geophys. Res.*, *92*, 7606, 1987.

Gussenhoven, M. S., D. A. Hardy, and W. J. Burke, DMSP/F2 Electron observations of equatorward auroral boundaries and their relationship to magnetospheric electric fields, *J. Geophys. Res.*, *86*, 768, 1981.

Gussenhoven, M. S., D. A. Hardy, and N. Heinemann, Systematics of the equatorward diffuse auroral boundary, *J. Geophys. Res.*, *88*, 5692, 1983.

Hardy, D. A., M. S. Gussenhoven, and E. Holeman, A statistical model of auroral electron precipitation, *J. Geophys. Res.*, *90*, 4229, 1985.

Knipp, D. J., F. K. Chun, M. G. McHarg, and F. J. Rich, An assessment of the midnight auroral boundary index (ABI) for use in global joule heating estimates, *Eos Suppl.*, *79*, 45, F666, 1998.

Siskind, D. E., C. A. Barth, D. S. Evans, and R. G. Roble, The response of thermospheric nitric oxide to an auroral storm, 2., Auroral latitudes, *J. Geophys. Res.*, *94*, 16,899, 1989

Siskind D. E., C. A. Barth, and J. M. Russell III, A climatology of nitric oxide in the mesosphere and thermosphere, *Adv. Space Res.*, *21*, 1353, 1998.

Solomon, S. C., et al., The Student Nitric Oxide Explorer, *Proc. SPIE*, *2810*, 121, 1996.

Stevens, M. H., R. R. Conway, J. G. Cardon, and J. M. Russell III, MAHRSI observations of nitric oxide in the mesosphere and lower thermosphere, *Geophys. Res. Lett.*, *24*, 3213, 1997.

S. C. Solomon and C. A. Barth, Laboratory for Atmospheric and Space Physics, University of Colorado, Boulder, CO 80309-0590 (e-mail: solomon@lasp.colorado.edu)

S. M. Bailey, Center for Atmospheric Sciences, Hampton University, 23 Tyler St., Hampton, VA 23668